

Modeling of Ship Propulsion Performance

Benjamin Pjedsted Pedersen (FORCE Technology, Technical University of Denmark)

Jan Larsen (Department of Informatics and Mathematical Modeling, Technical University of Denmark)



Full scale measurements of the propulsion power, ship speed, wind speed and direction, sea and air temperature, from four different loading conditions has been used to train a neural network for prediction of propulsion power. The network was able to predict the propulsion power with accuracy between 0.8-2.8%, which is about the same accuracy as for the measurements. The methods developed are intended to support the performance monitoring system SeaTrend® developed by FORCE Technology (FORCE (2008)).

KEY WORDS

Propulsion; performance; monitoring; non-linear neural network regression; neural networks; fuel consumption

INTRODUCTION

As part of the Industrial PhD project "Ship Performance Monitoring" automatic data sampling equipment was installed on the tanker "Torm Marie" in January 2008 and so far data from four different loading conditions are available.

Modeling of these loading conditions are fundamental to achieving a good solution. In the future, the variation in draught and trim will be added as variables.

Ship propulsion performance (referred to as the performance) is a measure of the energy consumption at a certain state, i.e. speed, loading condition, weather condition and other factors. During the lifetime of the ship the performance will decrease e.g. the fuel consumption will increase at a certain state or the speed will decrease at a certain power setting. This is mainly due to fouling of the hull and propeller. A typical trend of the speed reduction is illustrated in Figure 1.

Hence, performance evaluation is about comparing the fuel efficiency or propeller power at one time to another time, in other words to compare the ship at one state with another state. Since a ship is subjected to external factors such as wind, waves, shallow water, change in sea water temperature, etc. as illustrated in Figure 2, it is unlikely that the ship will ever be in the exact same situation more than once. Furthermore these external factors can be difficult to measure accurately and thus a similar situation will not be detected.

This deterioration is only a few percent and is therefore difficult to detect with traditional performance monitoring methods.

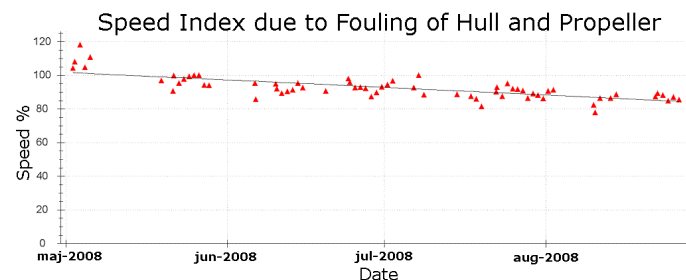


Figure 1: Increase of the fuel consumption as an effect the fouling

Traditionally, the problem has been solved by calculating a theoretical propulsion power for the actual condition using standard empirical resistance and propulsion methods, for example Harvald, S. A. (1983) or Holtrop, J. (1984) methods. For the estimation of the wind resistance a method proposed by Isherwood, R. (1972) can be used if no wind resistance coefficients are available for the ship.

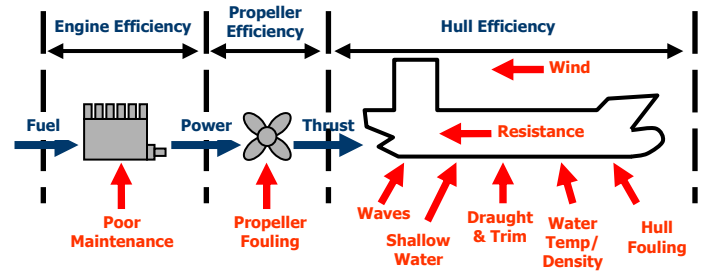


Figure 2: Performance variables

These empirical methods are derived from model tests and sea trials, and since most model test are carried out in a design condition (even keel) and speed, this is the region where it should be applied. In operation the ship will travel in many other conditions i.e. ballast draught and trimmed conditions.

Consequently these methods give a rough estimate of the propulsion power rather than an accurate reference point. If some measured values from model tests or sea trials are available, they can be used to adjust the empirical data and thus give a more accurate result.

Another part of the problem is to have sufficient input data for the analysis in order to capture the dynamics of the propulsion power. This is relevant for the traditional method and any other method that can be used. A short description of the input is given below:

Draught and trim - usually these fundamental variables for the power estimation are found from visual observation or from the loading computer before departure; sometimes the arrival condition is determined by observations, but usually only from the loading computer. Some ships are equipped with dynamic draught measuring devices, but these are very sensitive devices which deliver a signal with a significant variance. Draught and trim have approximately an accuracy of 0.2m, as that is the usual scale for draughts marks.

Power measurement - the power can be measured in different ways. Measuring the propeller shaft torque with a torsionmeter, and the rate of revolution with a tachometer will give the direct power delivered to the propeller and is thus the preferable method.

The main engine fuel consumption is also a fairly good measurement, but it is necessary to have sufficient information of the fuel quality. A change in the main engine performance will also show a change in the fuel consumption, so it can be difficult to determine the propeller and hull performance from the fuel performance alone.

Speed through the water - is measured by the speed log that is based upon the Doppler principle. Experience shows that the signal from the speed logs has a tendency to drift and hence many ship officers do not trust the speed logs. It is also possible to estimate the speed through the water from the sea current determined by a meteorological prognosis and from the speed

over ground given by the GPS navigator. Although the speed log can drift it is expected to give more reliable results than the one estimated from the sea current and GPS speed.

Relative wind speed and direction - is measured by a doppler anemometer Airmar® Weatherstation™ PB100 mounted on top of the superstructure. At this position the wind speed and direction is altered from the free stream wind due to the presence of the ship. Traditional methods for estimating the wind resistance is based on wind tunnel tests and hence assumes that the wind speed and direction is undisturbed. Since the undisturbed wind speed and direction is unknown from measurements, the measured (disturbed) values are used directly in the empirical model, although this is not correct. Furthermore, the wind resistance coefficients are in this case determined empirically, which induce additional uncertainty.

Air temperature - is also measured by the Airmar® Weatherstation™ PB100 unit. The air temperature can vary significantly within a few hours, which has a direct effect on the air density and consequently on the ship resistance, e.g. for the ship traveling with a speed of 15 knots in 10 m/s and 0°C headwind the air resistance will be 215kN and total resistance 953+215 = 1168 kN, for the ship and wind speed, but with an air temperature of 10°C the wind resistance is 199kN and the total resistance 953+199 = 1152 kN. The difference in air density has a relative influence on total resistance of (1168-1152) / 1168 = 1.4%. For the present measurement the air temperature varies between 24.5-28.8°C and has a variance of ~0.47.

Sea water temperature - is usually measured once daily by the engine crew. The seawater temperature has a significant impact on the sea water density and viscosity, and consequently on the resistance. The difference between sailing in 0°C and 30° C seawater results in a frictional resistance around 7%, and for the present type of ship the frictional resistance accounts for 90% of the total resistance.

Traditional Performance Evaluation

Traditionally the performance has been evaluated by rather simple procedures, where the daily fuel consumption has been reported in the "Noon Report" together with distance traveled over the last 24 hours, the corresponding average observed speed and a single weather observation.

This method gives a limited number of observations since there is a maximum of 365 observations per year. Then the days in port are deducted, together with observations including maneuvering, shallow water and significant changes in speed or heading. This might leaves 200 observations per year, each with only one weather observation which introduces a significant uncertainty, since the weather can change considerably during 24 hours.

SHIP PROPULSION THEORY

Classical ship propulsion procedures can be used as a reference point for the model. In these models the effects of ocean waves

have been neglected due to the uncertainty of both the estimate, the added resistance from the waves and measuring the actual wave height and period.

The total resistance thus consists of the still water resistance R_{SW} and the wind resistance R_{wind} .

Resistance

First, the still water resistance is found using the following equation:

$$R_{SW} = \frac{1}{2} C_{tot} \rho_{SW} S U^2 \quad (1)$$

The coefficient C_{tot} is defined as:

$$C_{tot} = C_v + C_R + C_A + C_{AA} \quad (2)$$

Where:

C_v , Viscous resistance coefficient: Defined as $C_v = C_f (1+k)$ where the frictional part C_f is determined from the formula:

$$C_f = \frac{0.075}{(\log_{10}(R_e) - 2)^2} \quad (3)$$

$$R_e = \frac{L_{wl} U}{\nu} \quad (4)$$

Where:

R_e is the Reynolds

k is the form factor that accounts for 3D flow effects around the hull, usually in the region 0-0.25.

C_R , Residual resistance coefficient is mainly accounting for the energy radiated by waves made by the ship. C_R can be estimated empirically by e.g. Harvald, S. A. (1983) or Holtrop, J. (1984), but the discrepancies can be up to 50% possibly making C_R the most difficult variable to determine in ship resistance.

C_A , Incremental resistance coefficient, accounts for differences in the hull roughness of the model and the ship. It is usually constant and in the region of 0.15-0.55 10^{-3}

C_{AA} , Allowance includes air and steering resistance.

Wind Resistance

In almost all conditions the hull and superstructure of the ship will result in a resistance component from the relative wind (the resistance can be negative, in case of strong following winds!). The wind resistance is calculated by

$$R_{wind} = \frac{1}{2} C_x \rho_{air} A_T V_R^2 \quad (5)$$

Where the wind resistance coefficient C_x , is determined empirically, by e.g. Isherwood, R. (1972), or by model tests, and vary with the relative wind direction, γ_R . A_T is the transverse projected area above the waterline and V_R is the relative wind speed. The wind coefficient C_x assumes that the wind speed and direction is undisturbed by the ship, which naturally is impossible for the on-board measurements.

Propulsion

The efficiency of the propeller η_D behind the ship is found by combining the results from model tests of the propeller alone, the so called open water test and model tests of the ship, with and without the propeller. If model tests are not available the values, wake fraction, w , thrust deduction, t , and relative rotative efficiency can be estimated by e.g. Harvald, S. A. (1983) or Holtrop, J. (1984). This results in the overall propulsion efficiency η_D .

Using the above described methods with the empirical method by Harvald, S. A. (1983) the propulsion power has been calculated for the measured conditions. This is illustrated in Figure 3.

Assuming that the ship is sailing in calm and deep water (depth/draught > 8), the propulsion power can thus be written as:

$$P_D = \eta_D^{-1} U (R_{SW} + R_{wind}) \quad (6)$$

A non-linear method has been developed based on the relation in (5), but did only show slightly better results than a similar linear method. Both the linear and non-linear method resulted in a relative error above 5% and was quickly discarded.

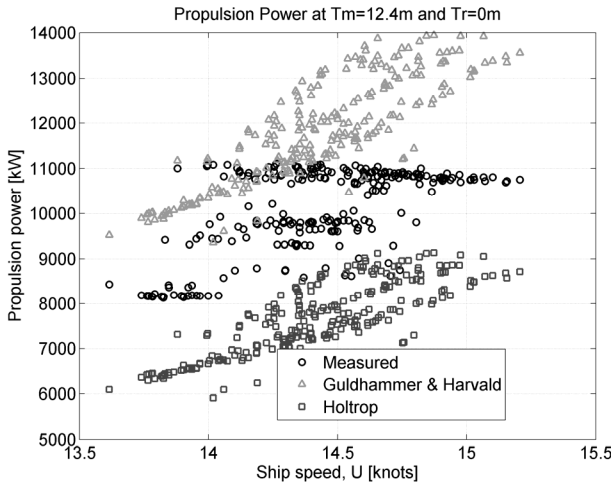


Figure 3: Propulsion calculation by empirical calculations, for data set #1 (Table 1), where Tm is the mean draught and Tr is the trim.

ARTIFICIAL NEURAL NETWORK

An artificial neural network (ANN) is an advanced form of non-linear regression that can be used to model complex relationships between input and output variables. ANN can be described as linear combinations of nonlinear regression models, with nonlinear basis functions, z_j .

$$y(x) = \sum_{j=0}^M w_{kj}^{(2)} z_{kj} \quad (7)$$

$$z_j = g \left(\sum_{i=0}^d w_{ji}^{(1)} x_i \right) \quad (8)$$

Where:

x are the measured input data.

y are the output, in this case the propulsion power

The network being used for this problem is a so called one hidden layer (z_1-z_M). Figure 4 illustrates an equivalent network with multiple output variables, whereas the present method only uses one output (y_1).

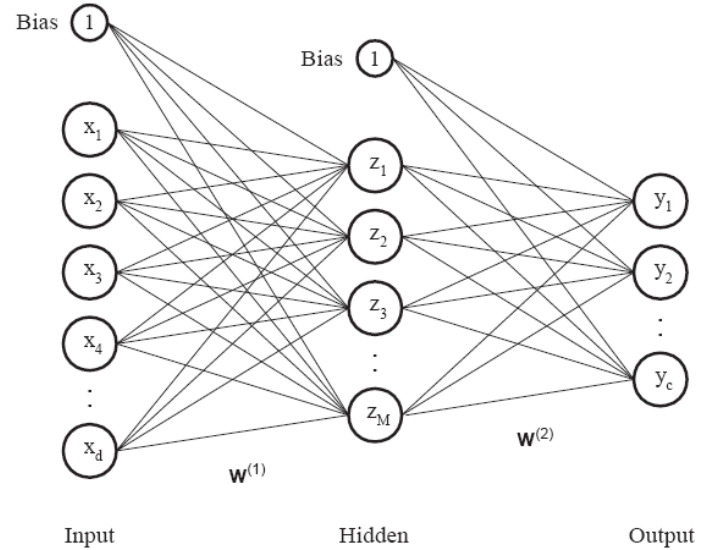


Figure 4: A single hidden layer artificial neural network, with multiple outputs.

The network is a non-linear regression model with additive Gaussian noise and trained with a Bayesian learning scheme.

After different attempts of modeling the propulsion power by using the physical and empirical relation, a neural network was tested and immediately showed surprisingly good results. Using a neural network efficiently thus requires sufficient input variables, hidden units, as well as a sufficient amount of data to train with.

From the physical relations of the ship propulsion theory the most important variables for the propulsion power, P , can be deducted to: ship speed, U , wind speed, V_R and direction, γ_R , air temperature, T_{air} and seawater temperature, T_{SW} .

Consequently the input and output variables are defined as:

$$x = [U \quad V_R \quad \gamma_R \quad T_{air} \quad T_{SW}]$$

$$y = P$$

The relationship between the different variables and the propulsion power is also known to a certain extent, e.g. the power is expected to be proportional to the ship speed cubed.

TEST DATA SET

The data has been collected onboard the 110,000 dwt tanker “Torm Marie” where a number of measurement were continuously logged, from where only the relevant data for this problem has been taken. The sampling was split into intervals of 10 minute time series with 10 minutes intervals. The sampling frequency of the times series was 1 second, but many of the measurements had inconsistent signals, i.e. sometime more than 10 second intervals. Power and speed were more or less consistently updated every 13 seconds.

Naturally the recorded data included samples from non-stationary situations as well as situations with zero forward speed. One significant variable to the variations in the samples was the change of heading. Even small changes (less than 1°) of the heading, had significant influence on the measured propulsion power. Samples with excessive variance in the heading have thus been excluded.

The sea state has a significant influence on the ship resistance and hence the propulsion power. No direct measurements of the sea state have been made, but the wind driven waves can be represented by the true wind speed to a certain extent. Making this assumption the swell is not included.

In Table 1 the key figures for each dataset are outlined. It is noted that the ship speed intervals are approximately in the same region for each sample. The distributions of the ship and true wind speed are illustrated in Figure 5-Figure 8. It should be noted that the Beaufort wind force (BF) 5 starts at approximately 16 knots wind speed. In this condition the wind driven waves are around 2 m high, which is when the sea state starts to influence the added resistance. From Figure 5 and Figure 6 it is noted that only a few occurrences are above this level and thus data sets #1 and #2 can be regarded as calm water conditions. Data set #3 and #4 on the other hand has a more significant contribution of measurements above BF 5 and the added resistance must be regarded as an extra contribution.

Table 1: Trained data sets, where N represents the number of 10 minute recording windows

Data set	Number of Samples	Mean draught, T_m	Trim Ta-Tf	U_{min} - U_{max}	P_{min} - P_{max}
M	N	[m]	[m]	[knots]	[kW]
1	238	12.4	0.0	13.6-15.2	8139- 11111
2	236	7.4	2.4	14.3-16.2	7574- 11283
3	142	7.85	2.7	13.6-15.2	7750-9248.5
4	63	12.15	0.0	13.4-16.1	9764- 11216

The input data are the mean values of the 10 minutes time series. In order to justify this, spreading of the signal has been

analyzed, for the ship speed, U , propulsion power, P and apparent wind speed, V_R . The air temperature has been neglected since it is very stable. For every 10 minute period the relative standard deviation, $(\sigma_{x,n}/\mu_{x,n})$ has been found and for every dataset the average of the relative standard deviation, $\bar{\sigma}_M$ has been determined:

$$\bar{\sigma}_{x,M} = \sqrt{\frac{1}{N} \sum_{n=1}^N \left(\frac{\sigma_{x,n}}{\mu_{x,n}} \right)^2} \quad (9)$$

Where:

- $\sigma_{x,n}$ is the standard deviation for the n 'th time series
- $\mu_{x,n}$ is the mean value for the n 'th time series
- x indicate the input/output variable (U, P, V_R, γ_R)

Similarly the average of the relative standard deviation $\mu_n, \bar{\mu}_{x,M}$, can be found.

$$\bar{\mu}_{x,M} = \frac{1}{N} \sum_{n=1}^N \left| \frac{\sigma_{x,n}}{\mu_{x,n}} \right| \quad (10)$$

The average of the relative standard deviation $\bar{\mu}_{x,M}$ and the average of the relative standard deviation $\bar{\sigma}_{x,M}$ are shown for every dataset in Table 2 and Table 3. It is noted that both the measured power and ship speed are all less than 1, but for the wind speed there are significant variations.

Table 2: The average of the relative standard deviation

M	N	$\bar{\mu}_U$	$\bar{\mu}_P$	$\bar{\mu}_{V_R}$
1	238	0.6%	0.8%	10.0%
2	236	0.6%	0.7%	18.0%
3	142	0.6%	0.6%	12.4%
4	63	0.6%	1.0%	7.9%

Table 3: The standard deviation of the relative standard deviation

M	N	$\bar{\sigma}_U$	$\bar{\sigma}_P$	$\bar{\sigma}_{V_R}$
1	238	0.2%	0.4%	5.9%
2	236	0.3%	0.2%	13.7%
3	142	0.2%	0.2%	7.2%
4	63	0.3%	0.5%	4.8%

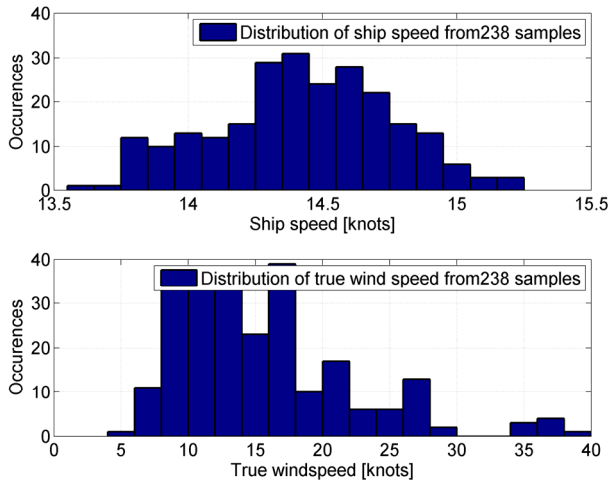


Figure 5: Ship speed and true wind speed distribution of sample #1

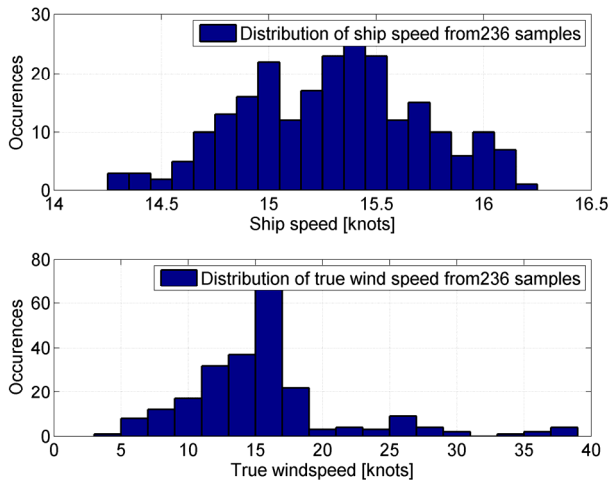


Figure 6: Ship speed and true wind speed distribution of sample #2

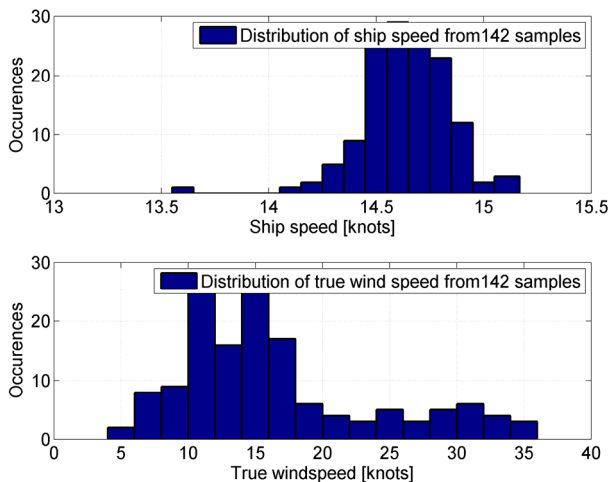


Figure 7: Ship speed and true wind speed distribution of sample #3

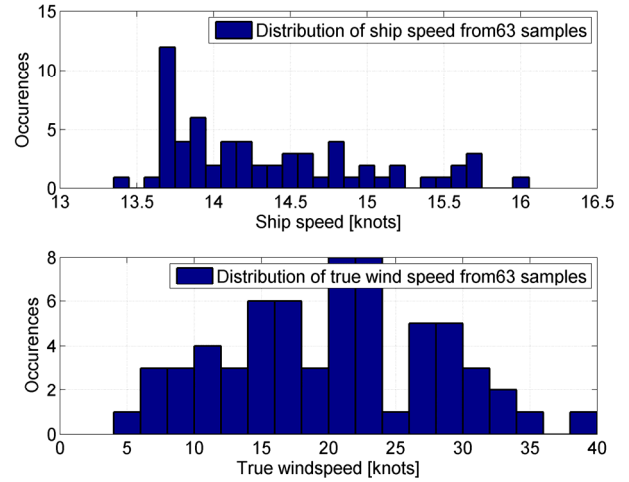


Figure 8: Ship speed and true wind speed distribution of sample #4

TRAINING

The training and test has been performed by a neural network (DTU toolbox (2002) Larsen, J. (1993), MacKay, D. J. C. (1992), Pedersen, M. (1997), Svarer, C.; Hansen, L. & Larsen, J. (1993))

The training procedure has been restarted 10 times in order to ensure that the network found the best possible solution for that particular case.

In order to cross validate, each data test set (1-4 in Table 1) has been divided into 5 training and test subsets, where 20% of the data set has been left only for testing and the remaining part for training. Before the subdivision the data set was permuted randomly.

In order to find the best number of hidden units the network has been trained with respectively 5, 10, 15 and 20 hidden units.

RESULTS

Due to the nature of the input data which is the mean values of the time series of 10 minutes, the resulting network is able to predict the mean propulsion power for a period of 10 minutes.

The results of each network have been evaluated by the relative sum of the errors squared, σ :

$$\tilde{\sigma} = \frac{\sum_{n=1}^N (\hat{P}_{test,n} - P'_{test,n})^2}{\sum_{n=1}^N P'_{test,n}{}^2} \quad (11)$$

The mean of the relative error has also been found in order to give more

$$\omega = \frac{1}{N} \sum_{n=1}^N \left| \frac{\hat{P}_{test,n} - P'_{test,n}}{P'_{test,n}} \right| \quad (12)$$

Where: $\hat{P}_{test,n}$ are the predicted values of the test data

$P'_{test,n}$ are the test samples from the cross validation set

N is number of test set

Every dataset set has been trained with a network 5, 10, 15 and 20 hidden units. Each of these networks has been trained five times in order to alternately use 20% of the data set for testing. In order to validate the results the cross validation error $\bar{\omega}$ and the cross validation error squared $\bar{\sigma}$:

$$\bar{\omega} = \frac{1}{K} \sum_{k=1}^{K=5} \omega \quad (13)$$

$$\bar{\sigma} = \frac{1}{K} \sum_{k=1}^{K=5} \tilde{\sigma} \quad (14)$$

Where K is the total number training/test set (5).

In Table 4 these two quantities are shown for each of the data sets. It is noted that data set #3 and #4 are much better results than #1 and #2, this is most likely because the limited dataset (142 and 63), are sampled around the same time, and thus have very little variation in the input variables. This is particularly pronounced in Figure 7 where the ship speed has been 14.5-5 knots about 90% of the time.

Taking this into account one should be careful using this network for ship speeds out of this range!

In the error plots of the best solutions, shown in Figure 9-Figure 12, the majority of the predictions are within an error of 500 kW. The prediction error distribution is illustrated in Figure 13-Figure 16, in the same plot a Gaussian distribution (shown as a blue line) has been generated using the mean value and the variance of the predicted errors. For #1 and #2 the normal distribution fits the histograms very well. For #3 the distribution is skewed due to a few outliers and for #4 the data set is most likely too small to be used, for this purpose, both #3 and #4 have a small spread, thereby justifying their use.

Table 4: Best results and related errors.

M	N	Mean draught	Trim Ta-Tf	No Hidden Units	cross validation error squared	cross validation error
		[m]	[m]		$\bar{\sigma}$	$\bar{\omega}$
1	238	12.4	0.0	20	0.13%	2.56%
2	236	7.4	2.4	15	0.15%	2.69%
3	142	7.85	2.7	20	0.03%	0.82%
4	63	12.15	0.0	20	0.04%	1.24%

Furthermore the cross validation error $\bar{\omega}$ and the cross validation error squared $\bar{\sigma}$ has been calculated for the two empirical performance evaluation methods, Harvald, S. A. (1983) and Holtrop, J. (1984). The results are shown in Table 5 and as expected these methods gives rather poor results compared with the data driven methods.

Table 5: Cross validation errors for the empirical methods.

M	N	Harvald, S. A. (1983)	Harvald, S. A. (1983)	Holtrop, J. (1984)	Holtrop, J. (1984)
		cross validation error squared	cross validation error	cross validation error squared	cross validation error
		$\bar{\sigma}$	$\bar{\omega}$	$\bar{\sigma}$	$\bar{\omega}$
1	238	3.63%	17.92%	6.13%	23.74%
2	236	7.47%	26.48%	8.18%	27.78%
3	142	5.68%	22.35%	7.93%	27.41%
4	63	10.75%	23.14%	9.70%	28.14%

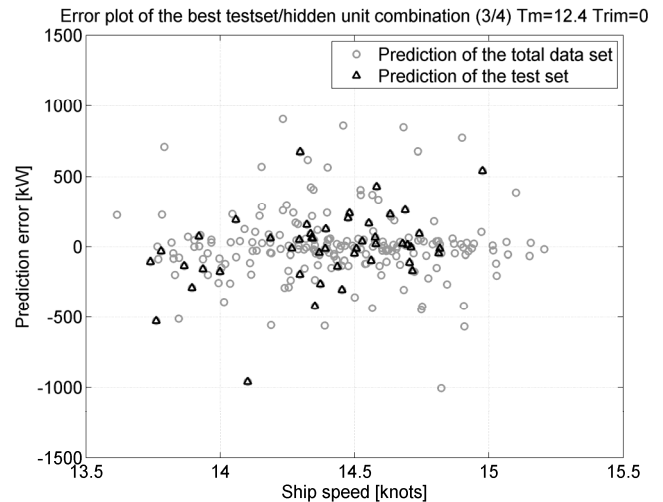


Figure 9: Prediction errors for sample #1

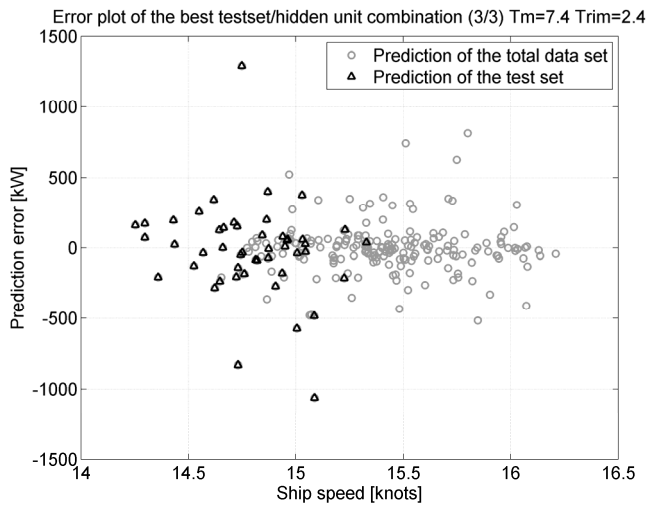


Figure 10: Prediction errors for sample #2

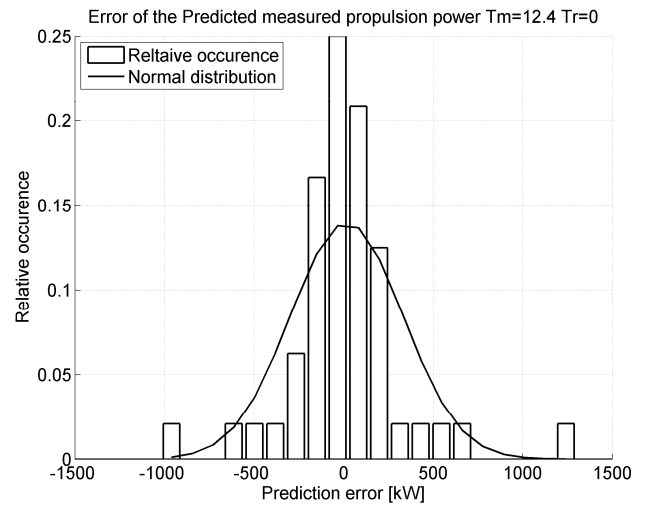


Figure 13: Relative distribution of the predicted errors for sample #1

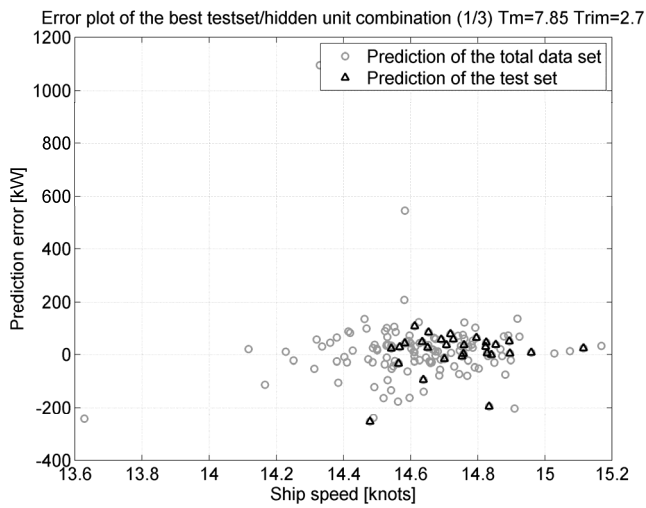


Figure 11: Prediction errors for sample #3

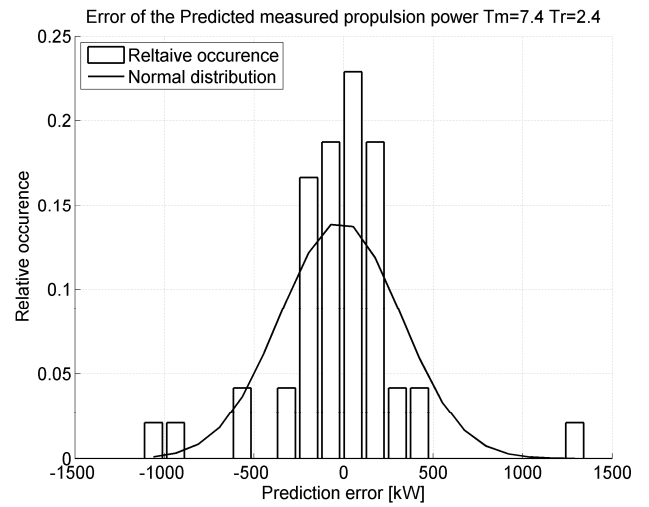


Figure 14: Relative distribution of the predicted errors for sample #2

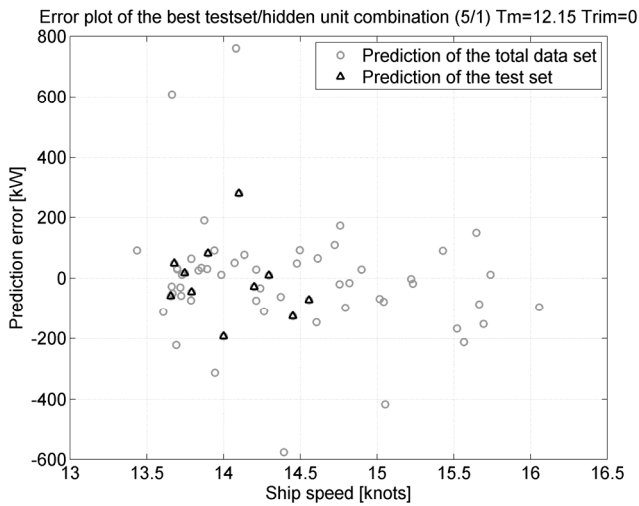


Figure 12: Prediction errors for sample #4

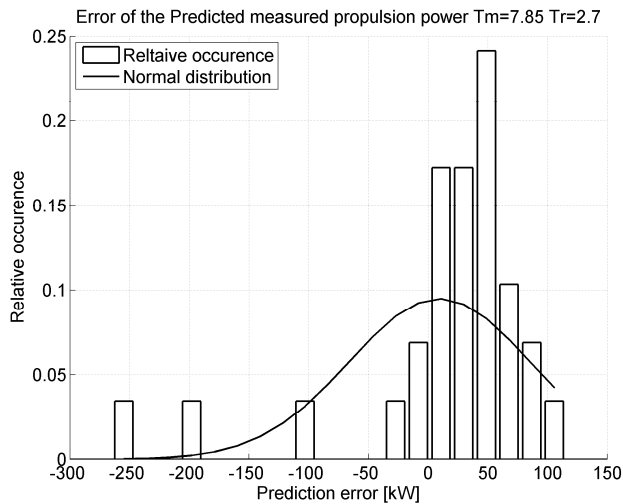


Figure 15: Relative distribution of the predicted errors for sample #3

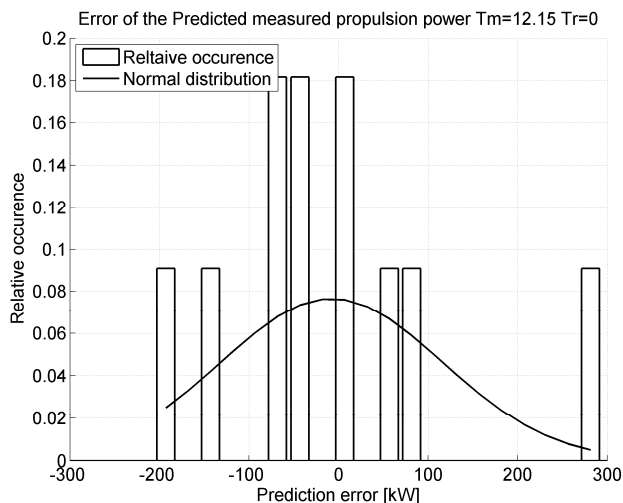


Figure 16: Relative distribution of the predicted errors for sample #4

CONCLUSIONS

It is possible to predict the propulsion power with a relative error of less than 2.7%, using a single hidden layer neural network while classical methods have a relative error of more than 5%. The prediction was carried out for four different states with the following input variables: ship speed, relative wind speed and direction, air temperature and sea water temperature. It is emphasized that the prediction should only be used with variables that lie within the training variable boundaries. As more data is collected onboard the vessel the model will gradually be extended.

ACKNOWLEDGEMENTS

Many thanks to the ship owner Torm and the crew onboard Torm Marie for letting me install the equipment and providing noon report data. In particular Chief Engineer Rasmus Hoffman, who has showed great interest in the project and been very

helpful monitoring the onboard system and sending data home. The work presented in this paper has been carried out during Pedersen's PhD study at FORCE Technology and the Technical University of Denmark, which is sponsored by The Danish Industrial PhD programme and Danish Centre of Maritime Technology (DCMT)/The Danish Maritime Fund.

REFERENCES

- FORCE (2008), SeaTrend® info sheet is available at: http://www.force.dk/en/Menu/Products+and+Concepts/Products/080220_seatrend.htm
- Harvald, S. A. (1983), *Resistance and Propulsion of Ships*, John Wiley & Sons.
- Holtrop, J. (1984), 'A Statistical re-analysis of resistance and propulsion data', *International Shipbuilding Progress* **31**, 272-276.
- Isherwood, R. (1972), 'Wind resistance of merchant ships', *Royal Institute of Naval Architecture*.
- ITTC (1978), 'ITTC – Recommended Procedures - Performance, Propulsion 1978 ITTC Performance Prediction Method', ITTC, 7.5-0203-01.4.
- DTU toolbox (2002), DTU toolbox: Neural regressor with quadratic cost function, <http://isp.imm.dtu.dk/toolbox>
- Larsen, J. (1993), 'Design of Neural Network Filters', PhD thesis, Electronics Institute, Technical University of Denmark.
- MacKay, D. J. C. (1992), 'A practical Bayesian framework for backpropagation networks', *Neural Computation* **4**, 448-472.
- Pedersen, M. (1997), 'Optimization of Recurrent Neural Networks for Time Series Modeling', PhD thesis, Institute of Mathematical Modeling, Technical University of Denmark.
- Svarer, C.; Hansen, L. & Larsen, J. (1993), On Design and Evaluation of Tapped-Delay Neural Network Architectures, in 'Proceedings of the 1993 IEEE International Conference on Neural Networks', pp. 46-51.